Hot rotating *fp* shell nuclei near proton drip

Mamta Aggarwal*
Nuclear Science Centre, Aruna Asaf Ali Marg, Post Box 10502, New Delhi 110067, India
(Received 31 October 2003; published 3 March 2004)

We investigate *fp* shell ($^{44-58}$Fe) nuclei in highly excited states. Effects of the thermal and rotational excitations on the separation energy are studied and it is found that these excitations affect the particle stability and alter the boundary of the proton drip line. The shell effects near the proton drip line are seen through the level density parameter a_e. Changes in the occupation probability as a function of temperature and spin are studied.

DOI: 10.1103/PhysRevC.69.034602 PACS number(s): 21.10.Dr, 24.60.−k, 23.50.+z, 21.60.−n

I. INTRODUCTION

The advent of Radioactive Ion Beam facilities and recent experiments on proton radioactivity [1–4] near proton drip line have made it possible to look closely into the structure and properties of the proton rich nuclei which are important both for nuclear physics and astrophysics. Study of proton rich nuclei, in particular those lying in *fp* shell region, is essential for understanding the interesting nuclear structure found in this region and certain astrophysical processes of nucleosynthesis by rapid proton capture. The path and the extent of the astrophysical processes can be determined by measuring the half lives, level density parameter, binding energies, separation energies, and mapping the precise location of proton drip line of proton rich *fp* shell nuclei.

Over the last decade, many attempts have been made for mapping the proton drip line experimentally [3,5] as well as theoretically [6–9], but only a few calculations have included the effects of excitation on the proton and neutron separation energies [10–12] and drip lines [13,14]. Incorporating the effects of excitations on the separation energy and drip line studies is necessary as these nuclei are formed usually in heavy ion collisions and are in highly excited state and their decay is greatly influenced by thermal and collective excitations. Therefore, we treat these nuclei in the framework of the statistical theory of hot rotating nuclei [15,16].

In the present work, we have chosen all the Fe isotopes from ^{44}Fe, a drip line nucleus to the most abundant stable isotope, ^{56}Fe, which provides one of the simplest systems expected to have a rotational structure [17]. The Fe isotopes have attracted the attention of several physicists [17,18] as Fe isotopes, being close to the spherical region of Ni isotopes, could be candidates for shape coexistence or shape transitions which are known in various other soft or transitional nuclei. These *fp* shell nuclei, lying between spherical magic gaps $N(\text{or } Z)=20$ to $N(\text{or } Z)=28$ play a very important role in our understanding of nuclear structure. Spin orbit splitting gives rise to a sizable energy gap in the *fp* shell between $f_{7/2}$ orbit and other orbits $(p_{3/2}, p_{1/2}, f_{5/2})$ making $N(\text{or } Z)=28$ a magic number, too. However, excitations across the gap are important for ground and excited state properties of many *fp* shell nuclei.

The locus of the neutron number for which the proton separation energy $S_P \rightarrow 0$ is the proton drip line. One proton separation energy is the energy required to knock out a proton from the last filled orbit which in this case is the closed shell orbit $f_{7/2}$ with two proton holes. To obtain the ground state one proton separation energy (S_P), we use the macroscopic-microscopic approach where we incorporate Strutinsky's shell correction to liquid drop model (LDM) mass formula [19] and obtain the corrected proton separation energy as in our earlier work [13]. In view of the high excitations possible in the nucleus formed in collisions, we introduce temperature and spin and find that the separation energy reduces as the thermal excitation energy increases, and as a result the drip line is pushed to higher neutron number. The level density parameter which carries deformation dependent shell effects in a natural way is investigated for various temperatures. Changes in the occupation probability with temperature and spin give a very clear picture about the changes taking place in the occupation of particles near the Fermi level.

II. Statistical theory of hot rotating nucleus

We start the statistical theory of hot rotating nucleus [15,16] with the grand canonical partition function of the superfluid system in terms of the single particle eigenvalues ϵ_i and the z component of the spin projection, m_i, of the deformed oscillator potential of the Nilsson Hamiltonian

$$Q(\alpha_Z, \alpha_N, \beta, \gamma) = \sum \exp(-\beta E_i + \alpha_Z Z_i + \alpha_N N_i + \gamma M_i). \tag{1}$$

The basic ingredient in the statistical theory is that a suitable shell model level scheme for various deformations is generated by assuming the nucleons to move in a deformed oscillator potential of the Nilsson Hamiltonian, diagonalized with cylindrical basis states [20,21] with the Hill-Wheeler [22] deformation parameter. The levels up to $N=11$ shells of the Nilsson model with Seegar parameters [23] are used. The single particle level schemes are different for protons and neutrons. The value of the angular deformation parameter θ ranges from −180° (oblate with symmetry axis parallel to the rotation axis) to −120° (prolate with symmetry axis perpen-

*Email address: drmamta@nsc.ernet.in

dicular to rotation axis). The axial deformation parameter δ ranges from 0 to 0.6.

The Lagrangian multipliers α, β, and γ conserve the particle number, total energy, and angular momentum of the system and are fixed by the following saddle point equations:

$$-\partial\, lnQ/\partial\,\beta = \langle E\rangle, \tag{2}$$

$$\partial\, lnQ/\partial\,\alpha_Z = \langle Z\rangle, \tag{3}$$

$$\partial\, lnQ/\partial\,\alpha_N = \langle N\rangle, \tag{4}$$

$$\partial\, lnQ/\partial\,\gamma = \langle M\rangle. \tag{5}$$

The corresponding equations in terms of single-particle levels for the protons ϵ_i^Z with spin projection m_i^Z and neutrons ϵ_i^N with spin projection m_i^N [24] are

$$\langle Z\rangle = \sum n_i^Z = \sum [1+\exp(-\alpha_Z + \beta\epsilon_i - \gamma m_i^Z)]^{-1}, \tag{6}$$

$$\langle N\rangle = \sum n_i^N = \sum [1+\exp(-\alpha_N + \beta\epsilon_i - \gamma m_i^N)]^{-1}, \tag{7}$$

$$\langle E(M,T)\rangle = \sum n_i^Z \epsilon_i^Z + \sum n_i^N \epsilon_i^N, \tag{8}$$

$$\langle M\rangle = \sum n_i^Z m_i^Z + \sum n_i^N m_i^N. \tag{9}$$

When $M=0$, the thermal excitation energy $U(T)$ of the system is given by

$$U(T) = E(0,T) - E(0,0), \tag{10}$$

where $E(0,0)$ is the ground state energy of the nucleus given by

$$E(0,0) = \sum \epsilon_i^Z + \sum \epsilon_i^N. \tag{11}$$

The rotational energy E_{rot} is calculated using Eq. (8):

$$E_{rot}(M) = E(M,T) - E(0,T). \tag{12}$$

As $T\rightarrow 0, E_{rot}$ corresponds to the yrast energy. We define an effective excitation energy

$$U_{eff}(T) = U(T) - \delta E_{shell}, \tag{13}$$

where part of the excitation energy is used to overcome the shell forces which are deformation dependent. The quantity δE_{shell} is the ground state shell correction obtained using Strutinsky's prescription [25]

$$\delta E_{shell} = \sum_{i=1}^{A} \epsilon_i - \tilde{E}, \tag{14}$$

the first term being the shell model energy in the ground state and the second term is the smoothed energy with the smearing width $1.2\hbar\omega$.

The total excitation energy is obtained as

$$U(M,T) = U_{eff}(T) + E_{rot}(M). \tag{15}$$

To evaluate the separation energy as a function of temperature and spin, we first calculate the binding energy and the ground state separation energy which is obtained using the macroscopic-microscopic approach as done earlier [13]:

$$\mathrm{BE}_{cor}(Z,N,\theta,\delta) = \mathrm{BE}_{LDM}(Z,N) - E_{def}(Z,N,\theta,\delta) - \delta E_{shell}(Z,N,\theta,\delta). \tag{16}$$

Here the total binding energy BE_{cor} has been obtained by incorporating the microscopic effects through Strutinsky's shell correction along with the deformation energy to the macroscopic binding energy obtained from the LDM mass formula. Then it is maximized with respect to the deformation parameters (θ,δ). The difference between BE_{cor} of parent and daughter nuclei gives the corrected proton separation energy

$$S_P^{cor} = \mathrm{BE}_{cor}(Z,N,\theta,\delta) - \mathrm{BE}_{cor}(Z-1,N,\theta,\delta). \tag{17}$$

A zero or negative separation energy indicates the instability of the nucleus against proton radioactivity.

In the case of excited nuclear systems we include the total excitation energy from Eq. (15) along with the deformation energy E_{def} to the total corrected binding energy and maximize it with respect to the deformation parameters θ and δ:

$$\mathrm{BE}(Z,N,T,M,\theta,\delta) = \mathrm{BE}(Z,N) - E_{def}(\theta,\delta) - U_{eff}(T,\theta,\delta) - E_{rot}(M,\theta,\delta). \tag{18}$$

One proton separation energy as a function of the thermal and rotational excitation is then obtained using

$$S_P(Z,N,T,M,\theta,\delta) = \mathrm{BE}(Z,N,T,M,\theta,\delta) - \mathrm{BE}(Z-1,N,T,M,\theta,\delta). \tag{19}$$

The single particle level density parameter $a_e(M,T)$ [26,27] as a function of angular momentum M and temperature T is found using

$$a_e(M,T) = U(M,T)/T^2. \tag{20}$$

III. RESULTS AND DISCUSSION

Figure 1 shows the variation of one proton separation energy [from Eq. (17)] of $^{44-58}$Fe as a function of the mass number A. Values of ground state S_P^{cor} (solid line) agree very well with the experimental [28] values and very recent theoretical predictions [9]. All the isotopes of Fe considered for this work are not very proton rich, nevertheless they are useful for a comparison of the model calculation with experimental data. ^{44,45}Fe are found unstable against proton decay with $S_P^{cor}<0$. ^{46}Fe is found to be the most proton rich stable nucleus (in agreement with theoretical prediction of RMF theory [8]) weakly bound with $S_P^{cor}=1.235$ MeV.

But, as thermal excitation is incorporated, the separation energy calculated using Eq. (19) (at $M=0$) decreases, and at certain excitation energies the separation energy reduces to 0 and the nuclei which were stable in the ground state become unstable against proton decay. In ground state ^{46}Fe was the

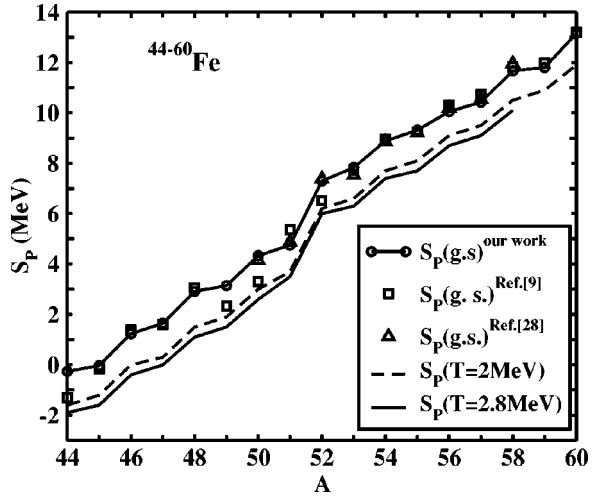

FIG. 1. Proton separation energy of $^{44-60}$Fe in ground state (g.s.) and in excited states for various temperatures.

most proton rich stable isotope of Fe but at $T=2$ MeV its $S_P=0$. At $T=2.8$ MeV, the separation energy of ^{47}Fe also reduces to 0 though it was bound with $S_P=1.651$ MeV in the ground state and 0.3 MeV at $T=2$ MeV. Thus with the thermal excitation, the exact location of the proton drip line has shifted to higher neutron number. Also, we come to know the exact excitation energy at which a particular stable nucleus will become unstable against proton emission.

Figure 2 shows deformation of some Fe isotopes vs A. Deformation and shape are determined by maximizing the total binding energy with respect to deformation parameters θ and δ [Eq. (18)]. At $T=1$ MeV, the shell effects are washed out and the equilibrium shape is spherical. Ground state deformations predicted here are quite close to the recent RMF theory predictions [29].

Figure 3 plots the level density parameter a_e calculated using Eq. (20) vs A. At low excitations, shell effects are predominant for *fp* shell proton rich Fe isotopes. For closed shell proton rich ^{46}Fe and ^{54}Fe nuclei a_e has much smaller

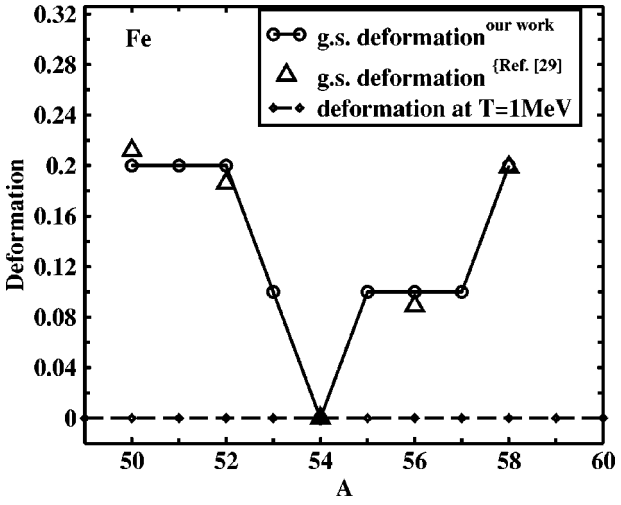

FIG. 2. Equilibrium deformation of $^{50-58}$Fe in ground state and excited state vs mass number A.

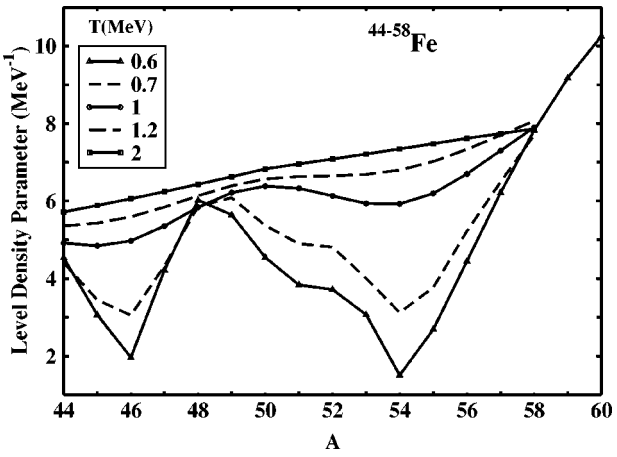

FIG. 3. Level density parameter a_e vs mass number A at different temperatures.

magnitude than other neighboring nuclei which are not closed shells. Figure 4 shows $K_e=A/a_e$ vs T for even-even $^{46-56}$Fe isotopes and we see that for $T<1.5$ MeV, K_e is very large and decreases very rapidly with T. With increasing excitation shell effects disappear and K_e attains almost a constant value. We have done calculations only for $0.6\ \text{MeV}<T<2.8$ MeV. Continuum corrections become important only after $T>3$ MeV as illustrated in Ref. [26], and are therefore not included here. However at low temperatures, our values of $K_e=A/a_e$ for ^{56}Fe are in close agreement with K_{se} of Ref. [26]. Here we also note that for a few Fe isotopes K_e is very small initially. This is due to deformation in those nuclei at low T. With increasing T, deformation decreases and K_e increases. At still higher T, these nuclei suffer a shape transition to spherical shape and then the variation of K_e with T follows the same pattern as for other nuclei as seen in the figure.

The rotational spectrum (in Fig. 5) of ^{46,50,54,58}Fe for spins up to $60\hbar$ shows the kinks in the curves due to the change in deformation and shape. As spin increases, the Fe isotopes considered here suffer a shape transition from spherical to oblate at around $M=20\hbar$ with small deformation $\delta=0.1-0.2$. Above $M=40\hbar$, the deformation rises up to $\delta=0.6$ with oblate shape ($\theta=-180°$).

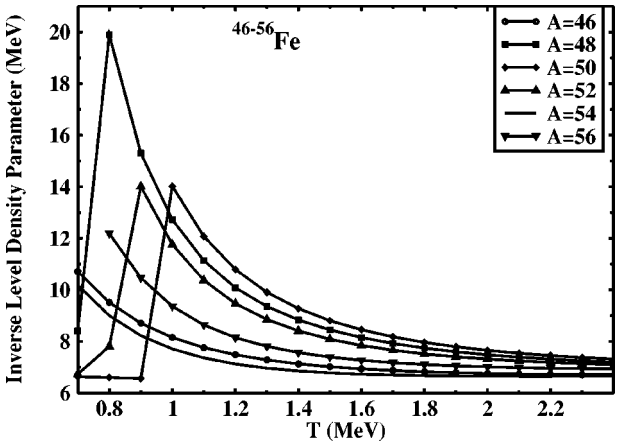

FIG. 4. Variation of K_e with temperature T for $^{46-56}$Fe.

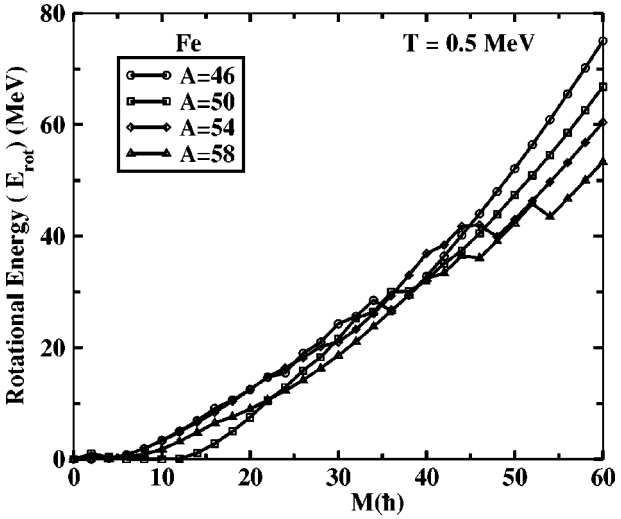

FIG. 5. Rotational spectrum of different Fe isotopes for spins from 0 to $60\hbar$.

Figure 6 shows the proton separation energy $S_p(M,T)$ [Eq. (19)] vs spin at $T=0.5$ MeV. The proton separation energy of ^{45}Fe, which was negative in the ground state, increases to a positive value 0.3 MeV at $M=22.5\ \hbar$ and goes up to 1.8 MeV at $M=60.5\ \hbar$. Therefore it is possible to get this nucleus stable with positive separation energy at the above mentioned excitations though it was unstable against proton decay in the ground state. From the figure we also note that ^{46}Fe has $S_P<0$ for certain spin values even at $T=0.5$ MeV.

The occupation probabilities (n_i) [see Eqs. (6) and (7)] of ^{46}Fe are displayed in Fig. 7 as a function of single particle energy ϵ_i for different temperatures and spins. At $T=0$, the occupation probability is unity up to the Fermi level and zero

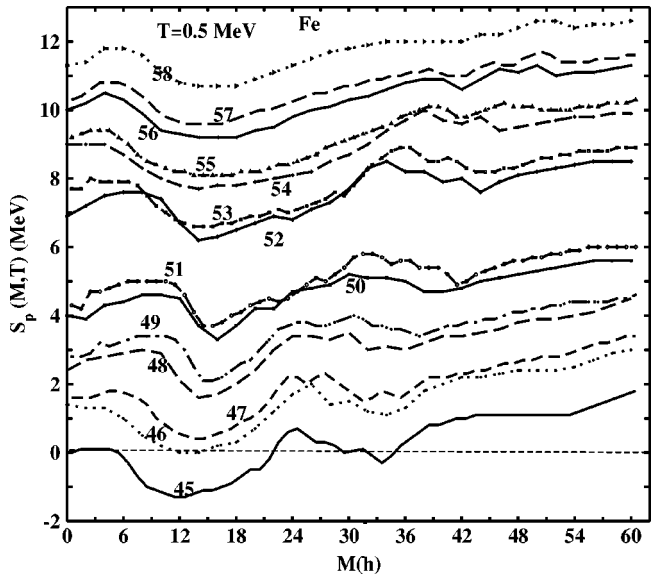

FIG. 6. One proton separation energy $S_P(Z,N,\theta,\delta,M,T)$ of $^{45-58}$Fe as a function of spin and temperature with $M=0$ to $60\hbar$, $T=0.5$ MeV. Numbers on the curves correspond to the mass number A.

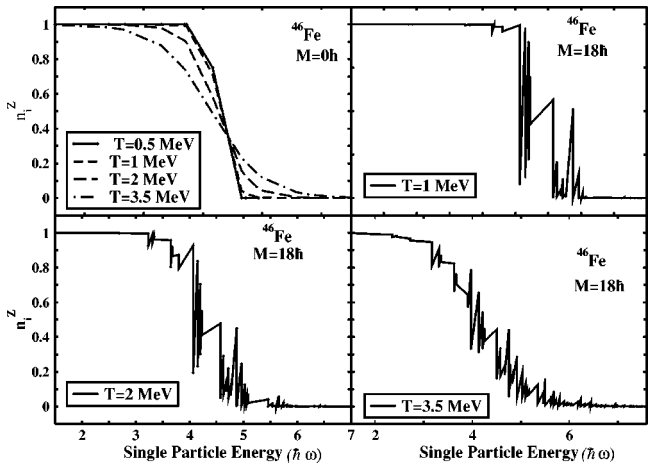

FIG. 7. Occupation probability n_i plotted for ^{46}Fe vs single particle energies ϵ_i for protons at various temperatures for spins $M=0$ and $M=18\hbar$.

beyond it. As the temperature increases, the occupation probability for levels below the Fermi level decreases from unity and for levels above the Fermi level increase from zero. This happens only for a few levels around the Fermi energy at lower temperatures but at higher excitations this happens for a large number of levels on both sides of the Fermi level. Particles from much lower levels get excited and occupation in much higher levels lying well above the Fermi level becomes possible. As the nucleons near the Fermi level are occupying much higher levels at high excitation, it becomes more likely that the outermost nucleon, which is very weakly bound with a very low separation energy, is thrown out of the nucleus. We also note that the fluctuations due to rotation are large at low T but only for a few levels around the Fermi level. As T increases fluctuations are smaller but extend to a larger area, i.e., farther away from the Fermi level below it and above it.

Figure 8 shows the occupation probabilities for ^{53}Fe and its residual nucleus ^{52}Mn and ^{46}Fe and ^{45}Mn after a proton emission. The n_i curve is almost the same around the Fermi level if there is no change in deformation and shape after the emission has taken place as in Fig. 8(b). Shape transition

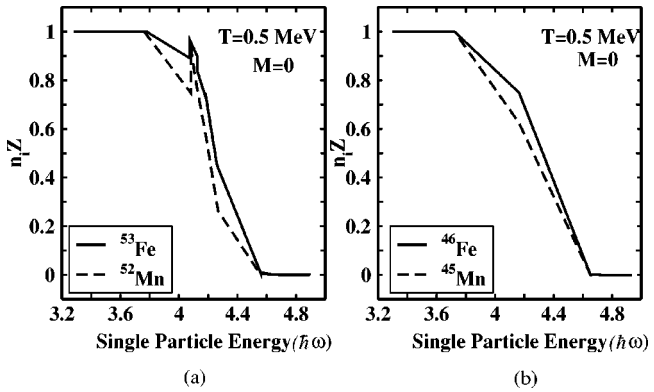

FIG. 8. n_i vs ϵ_i for protons for nuclei ^{53,46}Fe and their residual nuclei after one proton emission. Only few levels around Fermi level are shown in the figure.

occurs from triaxial ($\delta=0.1, \theta=-140°$) for ^{53}Fe to prolate ($\delta=0.1, \theta=-120°$) for ^{52}Mn.

IV. CONCLUSION

An elaborate study of the statistical properties of the *fp* shell Fe isotopes is done. They exhibit shell effects at the proton drip line. The magnitude of the level density parameter a_e is minimum at magic number drip line nucleus ^{46}Fe ($N=20$) and at stable nucleus ^{54}Fe ($N=28$). With increasing excitation, shell effects are washed out. The occupation probability and the separation energy of these nuclei vary with temperature and spin. Thermal and rotational excitation change the separation energy and alter the drip line. ^{45}Fe is a drip line nucleus in ground state but is found to be stable with positive separation energy at low temperature with $M>22\hbar$. ^{46,47}Fe are stable nuclei in ground state but decay by proton emission at thermal excitation corresponding to $T>2$ MeV.

ACKNOWLEDGMENTS

Financial assistance from The Council of Scientific and Industrial Research (CSIR), Government of India, is acknowledged. Useful discussions and suggestion from Dr. R. K. Bhowmik and Dr. S. K. Dutta of the Nuclear Science Centre are gratefully acknowledged. I thank Professor P. R. Subramanian for correcting the manuscript and giving useful suggestions.

[1] C. Detraz *et al.*, Nucl. Phys. **A519**, 529 (1990).
[2] V. Borrel *et al.*, Z. Phys. A **344**, 135 (1992); R. J. Irvine *et al.*, Phys. Rev. C **55**, R1621 (1997).
[3] M. F. Mohar, D. Bazin, W. Benenson, D. J. Morrossey, N. A. Orr, B. M. Sherrill, D. Swan, J. A. Winger, A. C. Mueller, and D. Guillemaud-Mueller, Phys. Rev. Lett. **66**, 1571 (1991).
[4] J. A. Winger *et al.*, Phys. Lett. B **299**, 214 (1993).
[5] F. Pougheon *et al.*, Nucl. Phys. **A327**, 17 (1987).
[6] W. E. Ormand, Phys. Rev. C **55**, 2407 (1991).
[7] R. Smolanczuk and J. Dobaczewski, Phys. Rev. C **48**, R2166 (1993).
[8] G. A. Lalazissis and S. Raman, Phys. Rev. C **58**, 1467 (1998).
[9] P. Moller and J. R. Nix, At. Data Nucl. Data Tables **66**, 131 (1997).
[10] M. Rajasekaran, T. R. Rajasekaran, N. Arunachalam, and V. Devanathan, Phys. Rev. Lett. **61**, 2077 (1988).
[11] M. Rajasekaran, T. R. Rajasekaran, P. Ratna Prasad, R. Premanand, D. Caleb Chanthi Raj, and V. Devanathan, Nucl. Instrum. Methods Phys. Res. B **79**, 286 (1993).
[12] M. Faber and M. Ploszajazak, Z. Phys. A **291**, 331 (1979).
[13] M. Rajasekaran and Mamta Aggarwal, Phys. Rev. C **58**, 2743 (1998).
[14] M. Rajasekaran and Mamta Aggarwal, Int. J. Mod. Phys. E **7**, 389 (1998).
[15] M. Rajasekaran, T. R. Rajasekaran, and N. Arunachalam, Phys. Rev. C **37**, 307 (1988).
[16] M. Rajasekaran, N. Arunachalam, and V. Devanathan, Phys. Rev. C **36**, 1860 (1987).
[17] H. Horie and K. Ogawa, Nucl. Phys. **A216**, 407 (1973).
[18] Huo Junde *et al.*, Nucl. Data Sheets **51**, 1 (1987).
[19] P. Moller and J. R. Nix, At. Data Nucl. Data Tables **26**, 165 (1981).
[20] G. Shanmugam, P. R. Subramanian, M. Rajasekaran, and V. Devanathan, *Nuclear Interactions*, Lecture Notes in Physics Vol. 72 (Springer, Berlin, 1979), p. 433.
[21] J. M. Eisenberg and W. Greiner, *Microscopic Theory of Nucleus* (North-Holland, New York, 1976).
[22] D. L. Hill and J. A. Wheeler, Phys. Rev. **89**, 1102 (1953).
[23] P. A. Seeger, Nucl. Phys. **A238**, 491 (1975).
[24] J. B. Huizenga and L. G. Moretto, Annu. Rev. Nucl. Sci. **22**, 427 (1972).
[25] V. M. Strutinsky, Nucl. Phys. **A95**, 420 (1967).
[26] B. K. Agrawal, S. K. Samaddar, J. N. De, and S. Shlomo, Phys. Rev. C **58**, 3004 (1998).
[27] J. N. De, S. Shlomo, and S. K. Samaddar, Phys. Rev. C **57**, 1398 (1998).
[28] A. H. Wapstra and G. Audi, Nucl. Phys. **432**, 55 (1985).
[29] G. A. Lalazisis, S. Raman, and P. Ring, At. Data Nucl. Data Tables **71**, 1 (1999).